Crystal Structure of Metastable Perovskite $Bi(Mg_{1/2}Ti_{1/2})O_3$: Bi-Based Structural Analogue of Antiferroelectric $PbZrO_3$

Dmitry D. Khalyavin,*[,†,‡] Andrei N. Salak,[†,‡] Nikolai P. Vyshatko,[†,‡] Augusto B. Lopes,[†] Nikolai M. Olekhnovich,[‡] Anatoly V. Pushkarev,[‡] Ivan I. Maroz,[‡] and Yury V. Radyush[‡]

Department of Ceramics and Glass Engineering, CICECO, University of Aveiro, 3810-193 Aveiro, Portugal, and Institute of Solid State and Semiconductor Physics, National Academy of Sciences, P. Brovka strasse 17, 220072 Minsk, Belarus

Received May 14, 2006. Revised Manuscript Received July 20, 2006

A metastable perovskite phase of $Bi(Mg_{1/2}Ti_{1/2})O_3$ composition (BMT) has been obtained under high-pressure (6 GPa) and high-temperature (1270 K) conditions. X-ray and electron diffraction studies have revealed a complex superstructure originating from antiferroelectric-like displacements of Bi^{3+} cations and octahedral tilting. A group theoretical analysis was used to enumerate the possible crystal structures compatible with both types of the distortions. On the basis of the symmetry arguments in combination with the diffraction methods, it has been concluded that the perovskite BMT is characterized by the orthorhombic *Pnnm* space group with unit cell parameters $a = 11.3207(10)$ Å, $b = 5.6433(10)$ Å, and $c = 7.8314(10)$ Å. A relation of the BMT crystal structure to that commonly accepted for antiferroelectric perovskite $PbZrO_3$ (PZ) is discussed.

Introduction

Ceramic ferroelectrics based on lead oxide are the most widely used as active elements of piezoelectric devices. $PbTiO_3$-constituent perovskite solid solutions with a morphotropic phase boundary (MPB) make up a majority of the actual market of piezoelectric materials.[1] Because of their excellent electromechanical properties, these materials, and particularlylead zirconate−titanate (PZT), had no environmentally friendlier alternative for a long time. A great number of systems including perovskite-related compositions were explored with the aim of attaining properties comparable to those of PZT. A lead-free substitute for PZT, in the form of textured ceramics based on sodium−potassium niobate, has recently been reported.[2] However, the prominent properties of these piezoceramics are achieved at the cost of extremely complicated processing. A search for new piezoelectrics is still topical, especially for the materials with an extended (to higher temperatures) operation range.[3]

Nowadays, bismuth-based compositions are widely considered as nontoxic substitutes for piezoelectric materials based on lead.[2,4] Indeed, Bi^{3+} and Pb^{2+} possess the same lone-pair electronic configurations and a majority of the Bi-containing oxygen octahedral compounds are known to demonstrate ferroelectric properties.[5] At the same time, because of the smaller size of Bi^{3+} as the *A*-site cation, only a few of the possible bismuth-based perovskite compositions could be obtained by conventional methods at normal pressure. The high-pressure technique allows us to extend a structure field of perovskite restricted by threshold magnitudes of the tolerance factor ($0.75 < t < 1.06$).[6] Moreover, complex oxide compositions ABO_3, which (because of some features of their chemical bond) favor less close-packed structures, can be transformed to perovskite structure under high pressure.[7] Attempts were made to obtain Bi-based analogues of PT and PZ using high-pressure synthesis. Belik et al.[8] has recently prepared high-pressure phases of $BiAlO_3$ and $BiGaO_3$. Dielectric properties of these compositions were not reported; however, their structural characteristics suggest that $BiAlO_3$ and $BiGaO_3$ can hardly serve in place of PZ and PT. Theoretical predictions of lead-free analogues of PZT have not been very successful so far.[9]

Systems of solid solutions PT-BiBO_3[10−11] and PT-Bi$(B',B'')O_3$[12−15] with MPB should be considered as being a

* To whom correspondence should be addressed. E-mail: dkhalyavin@cv.ua.pt.
† University of Aveiro.
‡ Institute of Solid State and Semiconductor Physics, National Academy of Sciences.

(1) Cross, L. E. *Nature* **2004**, *432*, 24.
(2) Saito, Y.; Takao, H.; Tani, T.; Nonoyama, T.; Takatori, K.; Homma, T.; Nagaya, T.; Nakamura, M. *Nature* **2004**, *432*, 84.
(3) Demartin Maeder, M.; Damjanovic, D.; Setter, N. J. *Electroceram.* **2004**, *13*, 385.
(4) Nagata, H.; Yoshida, M.; Makiuchi, Y.; Takenaka, T. *Jpn. J. Appl. Phys.* **2003**, *42*, 7401.
(5) Lines, M. E.; Glass, A. M. *Principles and Applications of Ferroelectric and Related Materials*; Oxford University Press: London, 1977.
(6) Goodenough, J. B.; Kafalas, J. A.; Longo, J. M. *Preparative Methods in Solid State Chemistry*; Hagenmuller, P., Ed.; Academic Press: New York, 1972; Chapter 1.
(7) Salak, A. N.; Shilin, A. D.; Bushinski, M. V.; Olekhnovich, N. M.; Vyshatko, N. P. *Mater. Res. Bull.* **2000**, *35*, 1429.
(8) Belik, A. A.; Wuernisha, T.; Kamiyama, T.; Mori, K.; Maie, M.; Nagai, T.; Matsui, Y.; Takayama-Muromachi, E. *Chem. Mater.* **2006**, *18*, 133.
(9) Baettig, P.; Schelle, C. F.; Le Sar, R.; Wagmare, U. V.; Spaldin, N. A. *Chem. Mater.* **2005**, *17*, 1376.
(10) Eitel, R. E.; Randall, C. A.; Shrout, T. R.; Rehrig, P. W.; Hackenberger, W.; Park, S. E. *Jpn. J. Appl. Phys., Part 1* **2001**, *40*, 5999.
(11) Eitel, R. E.; Randall, C. A.; Shrout, T. R.; Park, S. E. *Jpn. J. Appl. Phys., Part 1* **2002**, *41*, 2099.
(12) Randall, C. A.; Eitel, R.; Jones, B.; Shrout, T. R.; Woodward, D. I.; Reaney, I. M. *J. Appl. Phys.* **2004**, *95*, 3633.
(13) Suchomel, M. R.; Davies, P. K. *J. Appl. Phys.* **2004**, *96*, 4405.
(14) Snel, M. D.; Groen, W. A.; De With, G. *J. Eur. Ceram. Soc.* **2005**, *25*, 3229.
(15) Choi, S. M.; Stringer, C. J.; Shrout, T. R.; Randall, C. A. *J. Appl. Phys.* **2005**, *98*, 034108.

10.1021/cm061129w CCC: $33.50
Published on Web 09/09/2006

"low-lead" compromise. Atomic substitutions in a Bi-based end member of these systems can provide a variety of ferroelectric-like transition temperatures (T_C) and thereby a wider spectrum of operation ranges of the compositions in the vicinity of MPB.[14] It was reported that the position of MPB in the above-mentioned solid solutions can be estimated from the tolerance factor of a non-PT component;[13] however, there are other factors also affecting both T_C and MPB. These factors are mainly related to the peculiarities of its crystal structure. Therefore, in order to develop new MPB solid solutions with desired properties, direct data on crystal structure of their Bi-based end members are certainly needed. Moreover, detailed structure investigations of complex bismuth perovskites are of interest with respect to origin and behavior of dipole ordering in these compositions.

It seems that most of the $Bi(B',B'')O_3$ compositions considered as possible components of MPB solid solutions can be sintered only under high pressure. Inaguma et al. have recently reported on high-pressure preparation of perovskite ceramics $Bi(B'_{1/2}Ti_{1/2})O_3$ (B' = Co, Mg, Ni).[16,17] However, no structure refinement was performed, and the crystal symmetry of these Bi-based compositions was not clearly verified.

This work reports on high-pressure synthesis and crystal structure solution of metastable perovskite $Bi(Mg_{1/2}Ti_{1/2})O_3$ (BMT). The structure relation between BMT and PZ with respect to antiparallel shifts of *A*-site cations and oxygen octahedral tilting is discussed.

Experimental Section

Reagent-grade oxides Bi_2O_3, MgO, and TiO_2 were mixed according to the stoichiometric ratio and ball-milled in ethanol for 4 h. Some of the powders were then calcined at 1070 K for 4 h to study a phase formation in this system at a normal pressure. An equimolar mixture of Bi_2O_3 and $MgTiO_3$ was also attempted under the same conditions. Both the raw oxide mixture and the calcined powders were treated at high pressure and high temperature.

For high-pressure and high-temperature treatment, the powders were pressed into pellets 4.5 mm in diameter and about 4 mm in height. High-pressure synthesis at the ranges of 5−6 GPa and 1270−1370 K was performed in an anvil press DO-138A with a press capacity of 6300 kN. As-synthesized ceramics as well as those annealed in air between 670 and 1120 K were investigated.

Powder X-ray diffraction (XRD) data were collected at room-temperature using a Rigaku D/MAX-B diffractometer (Cu Kα radiation; tube power 40 kV, 30 mA; 2θ range 0−120°, step 0.02°, 20 s/step; graphite monochromator; receiving slit 0.30 mm). The Rietveld refinement of the obtained spectra was performed using the FULLPROF suite.[18]

The microstructure of the fractured surface and local chemical composition of the high-pressure ceramics after each annealing step were studied by scanning electron microscopy (SEM, Hitachi S-4100) equipped with an energy dispersive spectroscopy (EDS) detector.

The ceramics assigned for the transmission electron microscopy (TEM) observations were ground to about 30 μm and then milled until perforation using a BAL-TEC Ion Mill (RES 100). The samples were examined using a Hitachi H-9000 TEM operating at 300 kV.

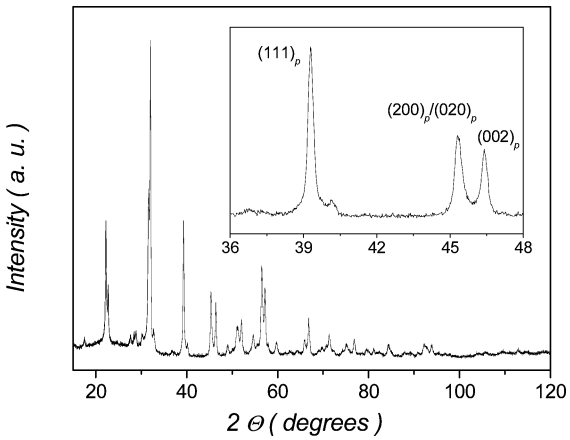

Figure 1. X-ray powder diffraction pattern of BMT. Inset shows the $(111)_p$ and $(200)_p$ normalized fundamental multiplets.

Results and Discussion

Before the high-pressure treatment, an attempt to synthesize perovskite BMT from the calcined powders was made using the conventional ceramic route. However, no trace of perovskite phase was detected in the reaction product. Different sintering conditions were attempted, but the resulting ceramics were non-single phase. The main phases were detected by XRD to be $Bi_{12}TiO_{20}$, $Bi_4Ti_3O_{12}$, and Mg_2TiO_4, whether calcined mixtures of the initial oxides or $Bi_2O_3 + MgTiO_3$ were used.

Perovskite BMT ceramics were synthesized at about 6 GPa and 1270 K regardless of the starting powders (Figure 1). The processing time did not exceed 5 min in all cases. Step-by-step annealing followed by XRD study has revealed an evolution of XRD spectra of the perovskite BMT phase. Increasing the annealing temperature from 670 to 870 K resulted in sharpening of the diffraction lines. Because of peculiar conditions of the high-pressure processing, mechanical stresses and defects of the crystal lattice could arise in ceramics during synthesis and quenching.[19] Both stresses and defects are known to broaden profiles of XRD peaks. It is believed that, when annealing, defects partly disappear and stresses are gradually released, resulting in the observed sharpening of the diffraction lines.

An annealing of BMT at 1020 K resulted in the decomposition of its perovskite phase. After thermal treatment at 1120 K for 2 h, any signs of the perovskite phase entirely disappeared. The resulting product was found to consist of the same set of the phases as that detected when sintering the initial powder at normal pressure.

SEM did not reveal any variation in grain-size distribution of the BMT ceramics until the annealing temperature exceeded 870 K. A microstructure with the characteristic grain size of about 100−200 nm that is typical of perovskite sintered under high pressure[19] was observed (Figure 2a). At

(16) Inaguma, Y.; Katsumata, T. *Ferroelectrics* **2003**, *286*, 111.
(17) Inaguma, Y.; Miyaguchi, A.; Katsumata, T. *Mat. Res. Soc. Symp. Proc.* **2003**, *755*, 471.
(18) Rodriguez-Carvajal, J. *Physica B* **1993**, *192*, 55.
(19) Olekhnovich, N. M.; Vyshatko, N. P.; Radyush, Yu. V.; Salak, A. N.; Ferreira, V. M. *J. Phys. Condens. Matter* **2003**, *15*, 6879.

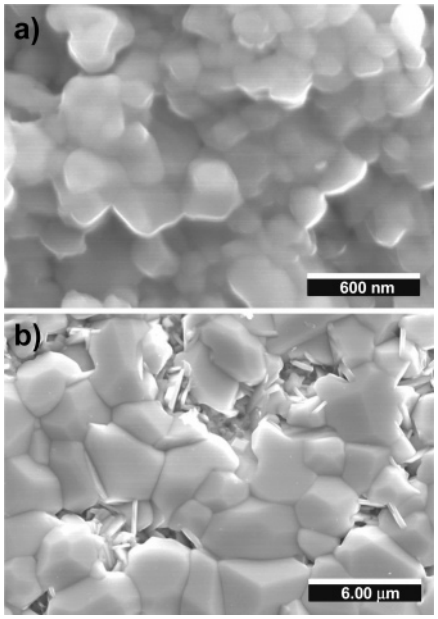

Figure 2. SEM observation of the fractured surface of BMT ceramics annealed at (a) 870 and (b) 1120 K.

the same time, the decomposition of BMT was found to be accompanied by a drastic change in the microstructure of the ceramics. As seen from Figure 2b, two types of grains developed in the ceramics annealed at 1120 K. The big grains were identified by EDS to consist mainly of $Bi_{12}TiO_{20}$, whereas the small elongated (stick-shaped) grains are composed of $Bi_4Ti_3O_{12}$ and Mg_2TiO_4.

On the basis of the thermal stability data on the BMT perovskite, we performed further structural characterization on the ceramics annealed at 870 K. Preliminary analysis of XRD pattern has revealed that the fundamental reflections $\{hkl\}_p$ are singlets in the case of $h = k = l$ and doublets with more intensive first line when $h = k \neq l$ (Inset in Figure 1). This observation is consistent with a tetragonal metric of the pseudocubic perovskite subcell where $a_p = b_p > c_p$ (a_p, b_p, and c_p are parameters of the subcell). Unlike La_2MgTiO_6,[20] the $1/2(111)_p$ superstructure reflection was not observed in the XRD pattern of BMT (inset in Figure 3), supporting a random distribution of Mg^{2+} and Ti^{4+} cations in a long-range scale. Nevertheless, higher-order reflections of the $1/2\{h, k, l = 2n + 1\}_p$ family ($h + k + l > 3$) with a low but visible intensity are present in the pattern (Figure 3). According to Glazer,[21] these reflections can be attributed to an antiphase octahedral tilting. Along with these, a set of additional reflections, which could not be indexed in a $2a_p \times 2b_p \times 2c_p$ supercell, was detected.

In order to determine the unit-cell dimension, we performed an electron diffraction experiment on numerous crystallites. As a result, a complex superstructure has been revealed in BMT (Figure 4). Two different variants of the $<100>_p$ zone axis electron diffraction patterns, ZAEDPs ((a) with and (b) without the superstructure) demonstrate that the psudocubic subcell is quadrupled along one of the $<110>_p$ directions. The $1/4\{hk0\}_p$ type superstructure is also seen in

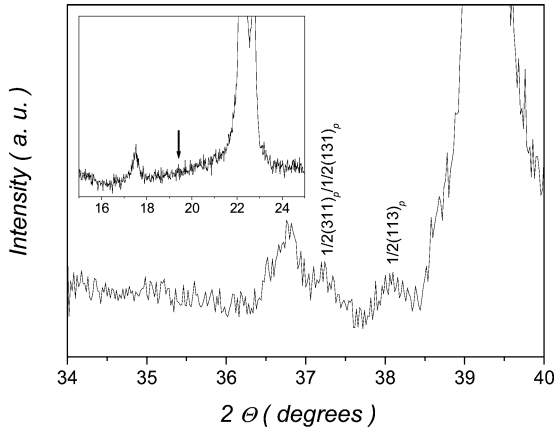

Figure 3. Part of the X-ray diffraction pattern with the $1/2(311 + 131)_p$ and $1/2(113)_p$ superstructure reflections. Inset shows the range where the $1/2(111)_p$ reflection is expected (the position is marked by arrow).

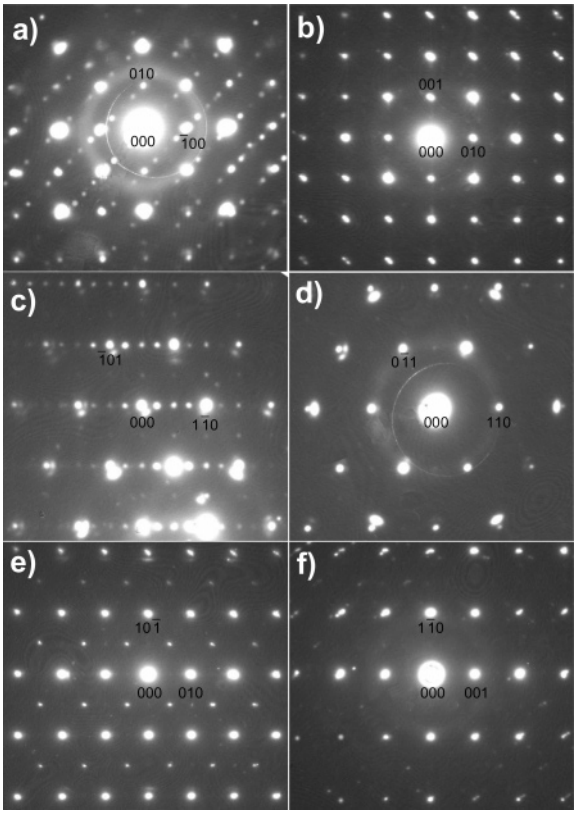

Figure 4. Electron diffraction patterns obtained from BMT with zone axes chosen as (a, b) $<100>_p$, (c, d) $<111>_p$, and (e, f) $<110>_p$.

some $<111>_p$ patterns (Figure 4c). Similar ZAEDPs have recently been obtained by Woodward and Reaney[22] from crystallites of PZ. The superstructure observed in PZ was attributed to antiferroelectric displacement of Pb^{2+} cations in the $[110]_p/[\bar{1}\bar{1}0]_p$ directions. Such displacement was shown to result in the *Pbam* space group with a $2\sqrt{2}a_p \times \sqrt{2}b_p \times c_p$ unit cell. Because Bi^{3+} and Pb^{2+} have similar electronic configurations with a $6s^2$ lone pair and strongly covalent chemical bonds, one can suggest by analogy that the shift of Bi^{3+} is the reason for the superstructure development in BMT. On the basis of the observed antiphase octahedral tilting, which doubles the pseuducubic subcell in all three

(20) Avdeev, M.; Seabra, M. P.; Ferreira, V. M. *J. Mater. Res.* **2002**, *15*, 1112.
(21) Glazer, A. M. *Acta Crystallogr., Sect. A* **1975**, *31*, 756.
(22) Woodward, D. I.; Reaney, I. M. *Acta Crystallogr., Sect. B* **2005**, *61*, 387.

directions, the orthorhombic $2\sqrt{2}a_p \times \sqrt{2}b_p \times 2c_p$ unit cell has been successfully applied for the indexation of the XRD pattern. Further inspection of ZAEDPs was undertaken to ascertain the octahedral tilt system presented in BMT. The absence of the $1/2\{h, k = 2n + 1; l = 2n\}_p$ superstructure reflections in some $<111>_p$ patterns (Figure 4d) allow one to rule out all the configurations involving in-phase octahedral tilting.[22] Traces of these reflections were not detected by XRD. At the same time, the reflections from antiphase octahedral tilting are present in some $<110>_p$ ZAEDPs (Figure 4e), in agreement with the XRD observations. As these reflections can superpose with those coming from a possible short-range ordering between Mg^{2+} and Ti^{4+} cations, a deduction of the appropriate tilt system is rather complicated. Nevertheless, because the $<110>_p$ ZAEDPs without the superstructure (Figure 4f) or with very weak intensity were observed, one can conclude that, at least for some of the grains, the effect of the cation ordering is negligible. Thus, taking into account the results of both X-ray and electron diffraction, it can be assumed that the crystal structure of BMT involves antiferroelectric-like displacements of Bi^{3+} cations and solely antiphase octahedral tilting.

In this stage, an analogy between the crystal structures of PZ and BMT can be drawn. Indeed, in both cases, the ferroelectrically active cations are displaced in the same way, the pseudocubic subcell is characterized by a tetragonal metric with $a_p = b_p > c_p$, and only the antiphase type of an octahedral tilting is present. Thereby, BMT should be considered as being a Bi-based structural analogue of PZ. The crystal structure of the latter is ordinarily described using the *Pbam* space group,[22,23] which is compatible with both the antiferroelectric displacements of Pb^{2+} cations and the two-tilted $a^0b^-b^-$ configuration (in the notation of Glazer[21]). However, it must be taken into consideration that the distortions caused by the *A*-site cation displacement are represented as vectors, whereas the distortions due to an octahedral tilting have a pseudovector character. A mutual orientation between the vector and the pseudovector plays an important role in the determination of a resulting symmetry, which was clearly demonstrated by Stokes et al.[24] from the result of a group theoretical analysis performed for octahedral tilting in ferroelectric perovskites. Although the authors analyzed the case of ferroelectric displacements of the B-site cation, the situation is similar to the present one, because both types of the distortions, vector and pseudovector, were involved. According to them, two different space groups, *Ima*2 and *Imm*2, correspond to $a^-_+ a^-_+ c^0_0$ and $a^-_+ a^-_- c^0_0$ tilt configurations. (Subscripts "+" and "−" denote cation displacements along a given axis). In these two cases, the orientations of the pseudovector and the polar vector are parallel and perpendicular to each other, respectively. A similar situation seems to be realized when combining the antiferroelectric-like displacements observed in BMT and PZ with an octahedral tilting. It takes actual such symmetry analysis to reveal an appropriate space group for BMT.

A group theoretical analysis has been performed with the aid of ISOTROPY software developed by Stokes and Hatch.[25] According to Howard and Stokes,[26] antiphase rotations of octahedra around the $<100>_p$ axis of the $Pm\bar{3}m$ space group are transformed as pseudovector basis functions of the R_4^+ (k = 1/2 1/2 1/2) three-dimensional irreducible representation. Vector relations between the orthorhombic *Pbam* and the cubic $Pm\bar{3}m$ space groups are expressed as

$$\vec{a} = 2\vec{a}_p - 2\vec{b}_p;\ \vec{b} = \vec{a}_p + \vec{b}_p;\ \vec{c} = \vec{c}_p;$$
or shorter (2, −2, 0) (1, 1, 0) (0, 0, 1) (1)

where $\vec{a}$, $\vec{b}$, $\vec{c}$, and $\vec{a}_p$, $\vec{b}_p$, $\vec{c}_p$ are lattice vectors of the orthorhombic and cubic unit cells, respectively. An analysis of the above relations allows one to conclude that the antiferroelectric-like shift of Bi^{3+} cations found in X-ray and electron diffraction experiments can be associated with the Σ_2 (k = 1/4 1/4 0) 12-dimensional irreducible representation of $Pm\bar{3}m$ with the *P*2(0, a, −a, 0, 0, 0, 0, 0, 0, 0, 0, 0) direction of the order parameter in representation space. By combining the R_4^+ and Σ_2 representations, we obtained a list of isotropy subgroups corresponding to the coupled order parameter. The results of the calculations are summarized in Table 1. Modified Glazer's notations for the tilt configurations were used that were similar to those introduced by Stokes et al.[24] for ferroelectric tilted perovskites. For example, a displacement along the $[110]_p$ direction can be represented by either $a^0_+ a^0_+ c^0_0$ or $a^0_- a^0_- c^0_0$ combinations because the distortions are of antiferroelectric type and there are shifts along both the $[110]_p$ and the $[\bar{1}\bar{1}0]_p$ directions. The superscripts have their usual (Glazer's) meaning.

Let us discuss the ideology of the tilt system assignment on the basis of an analysis of the order parameter direction. A projection of the coupled order parameter onto the R_4^+ subspace in all the cases coincides with the direction of the order parameter in the first distinct domain with the (E|000) generator of the corresponding isotropy subgroup. It means that a nonzero first, second, or third component of the coupled order parameter correspond to an antiphase octahedral tilting about *z*, *x* or *y* axes of the parent $Pm\bar{3}m$ space group, respectively. The projection of the coupled order parameter onto the Σ_2 subspace does not always coincide with the order parameter of the first distinct domain of the *Pbam* isotropy subgroup. In order to find the direction of the *A*-site cation displacements in respect to the basis of the $Pm\bar{3}m$ group, we should perform a particular analysis. As seen from Table 1, the *Pnma* space group appears with the *P*1(1)*P*2(1)(a, 0, 0, 0, b, −b, 0, 0, 0, 0, 0, 0, 0, 0, 0, 0) coupled order parameter. A nonzero first component corresponds to an octahedral tilting about the *z*-axis of the $Pm\bar{3}m$ space group. The direction of the order parameter in the Σ_2 subspace indicates that the first distinct domain of the *Pbam* with the (E|000) generator is under consideration. In this domain, the lattice vectors of the *Pbam* isotropy subgroup are (2, −2, 0) (1, 1, 0) (0, 0, 1) with regard to the $Pm\bar{3}m$. It means that *A*-site cations are displaced along

(23) Sawaguchi, E.; Maniwa, H.; Hoshino, S. *Phys. Rev.* **1951**, *83*, 1078.
(24) Stokes, H. T.; Kisi, E. H.; Hatch, D. M.; Howard, C. J. *Acta Crystallogr., Sect. B* **2002**, *58*, 934.
(25) Stokes, H. T.; Hatch, D. M. *ISOTROPY*; http://stokes.byu.edu/isotropy.html; 2002.
(26) Howard, C. J.; Stokes, H. T. *Acta Crystallogr., Sect B* **1998**, *54*, 782.

Table 1. Space Group Symbol (and number), Order Parameter, Tilt System, Lattice Vectors, and Origins of the Isotropy Subgroups with Respect to the Parent *Pm*$\bar{3}$*m* Group.

space group	order parameter $R_4^+ \oplus \Sigma_2$	tilt system	basis	origin
Pbam (No. 55)	(0,0,0,0,a,−a,0,0,0,0,0,0,0,0,0,0)	$a_+^0\ a_+^0\ c_0^0$	(2,-2,0)(1,1,0)(0,0,1)	(1/2,0,0)
Pnma (No. 62)	(a,0,0,0,b,−b,0,0,0,0,0,0,0,0,0,0)	$a_+^0\ a_+^0\ c_0^-$	(1,1,0)(0,0,2)(2,-2,0)	(1/2,0,1/2)
Pbam (No. 55)	(a,a,0,0,0,0,0,0,b,0,b,0,0,0,0,0)	$a_+^-\ b_0^0\ a_+^-$	(−2,0,2)(1,0,1)(0,2,0)	(0,1/2,1/2)
Pnnm (No. 58)	(a,a,0,0,0,0,0,0,b,0,b,0,0,0,0,0)	$a_+^-\ b_0^0\ a_-^-$	(2,0,2)(1,0,-1)(0,2,0)	(1,1/2,1/2)
$P2_1/c$ (No. 14)	(a,a,b,0,0,0,0,0,c,0,c,0,0,0,0,0)	$a_+^-\ b_0^-\ a_+^-$	(0,2,0)(−2,0,2)(1,0,1)	(0,1/2,1/2)
$P2_1/c$ (No. 14)	(a,a,b,0,0,0,0,0,c,0,c,0,0,0,0,0)	$a_+^-\ b_0^-\ a_-^-$	(0,2,0)(−1,0,1)(2,2,2)	(1/2,3/2,1)
*P*2/*m* (No. 10)	(a,b,0,0,0,0,0,0,c,0,c,0,0,0,0,0)	$a_+^-\ b_0^0\ c_+^-$	(2,0,-2)(0,2,0)(1,0,1)	(1,1/2,-1/2)
$P\bar{1}$ (No. 2)	(a,b,c,0,d,−d,0,0,0,0,0,0,0,0,0,0)	$a_+^-\ b_+^-\ c_0^-$	(0,0,2)(1,1,0)(−2,2,0)	(−1/2,1,1/2)

the $[110]_p/[\bar{1}\bar{1}0]_p$ directions. Therefore, the respective tilt system is $a_+^0\ a_+^0\ c_0^-$.

The *Pbam* space group appears with the *P*2(1)*P*2(3)(a, a, 0, 0, 0, 0, 0, 0, b, 0, b, 0, 0, 0, 0, 0) coupled order parameter. Nonzero components in the R_4^+ subspace are related to an octahedral tilting about the axes *z* and *x* of the *Pm*$\bar{3}$*m* with equivalent amplitudes. Nonzero components in the Σ_2 subspace indicate that the third distinct domain of the corresponding isotropy subgroup (*Pbam*) is activated. In this domain. the lattice vectors of the subgroup are (−2, 0, 2) (1, 0, 1) (0, 1, 0) with regard of the *Pm*$\bar{3}$*m* and consequently the directions of the *A*-site cation displacements are $[101]_p/[\bar{1}0\bar{1}]_p$. Therefore, this space group should be associated with the $a_+^-\ b_0^0\ a_+^-$ tilt configuration. Directions of the vector and the pseudovector coincide in this configuration.

The difference of the *Pnnm* space group with the *P*2(1)-*P*2(4)(a, a, 0, 0, 0, 0, 0, 0, b, 0, b, 0, 0, 0, 0, 0) coupled order parameter from the previous one is the direction of the order parameter in the Σ_2 subspace. In the given case, it coincides with the fourth distinct domain of the *Pbam* subgroup, where *A*-site cations are displaced along the $[10\bar{1}]_p/[\bar{1}01]_p$ directions. The adequate tilt system is $a_+^-b_0^0\ a_-^-$ with orthogonal mutual orientation of the vector and pseudovector. Other tilt configurations were identified in an analogous way.

On the basis of the possible space groups and tilt systems, we can analyze and discuss the likely crystal structure of BMT. First of all, some of the tilt systems from Table 1 can be immediately ruled out just reasoning from an examination of the diffraction data on the superstructure associated with the R_4^+ irreducible representation. The $a_+^0\ a_+^0\ c_0^-$ configuration (*Pnma*) is incompatible with the presence of the $1/2\{h, k, l = 2n+1; h = k\}_p$ reflections in the XRD pattern (Figure 3). An undetected superstructure in the $<110>_p$ ZAEDPs excludes the $a_+^-\ b_0^0\ c_+^-$ and $a_+^-\ b_+^-\ c_0^-$ configurations.[22] The remaining four tilt systems are consistent with the observed superstructure and additional arguments are required to make an appropriate choice.

In this situation, therefore, an analysis of expected metric of the pseudocubic subcell was carried out. The displacements of *A*-site cations along the $[110]_p/[\bar{1}\bar{1}0]_p$ directions without an octahedral tilting should result in a pseudomonoclinic subcell with $a_p = b_p > c_p$ and $\alpha_p = \beta_p = 90° \neq \gamma_p$ (α_p, β_p, and γ_p are the angles of the pseudocubic subcell). This metric allows the orthorhombic unit cell to be chosen as given by the eq 1. In this setting it is expected that $a/2 < b$. On the basis of an examination of the fundamental multiplets, one can arrive at the conclusion that the metric of the pseudocubic subcell is tetragonal. The tetragonality

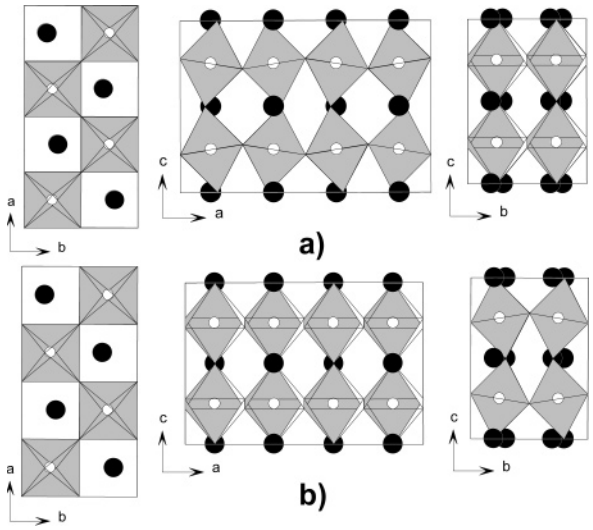

Figure 5. Polyhedral representation of the crystal structure corresponding to (a) *Pbam* space group and (b) *Pnnm* space group tilt configurations.

means that $a/2 = b$ in the orthorhombic unit cell. To satisfy this condition, a mechanism compensating the deviation of γ_p from 90° must be present. A tilting about all the three $<100>_p$ primitive axes in the cases of the $a_+^-\ b_0^-\ a_+^-$ and $a_+^-\ b_0^-\ a_-^-$ configurations with monoclinic space groups can tune γ_p to 90°, but should result also in $\alpha_p = \beta_p \neq 90°$ type of distortions. Because the XRD spectrum can be entirely indexed in the orthorhombic unit cell, there is not a necessity to involve the monoclinic symmetry. Hence, these tilt systems are unlikely. As a result of the above analysis, only two configurations, namely $a_+^-\ b_0^0\ a_+^-$ with the *Pbam* space group usually attributed to PZ and $a_+^-\ b_0^0\ a_-^-$ with the *Pnnm* space group should be further considered. A polyhedral representation of these two crystal structures is shown in Figure 5. As seen, these tilt systems are characterized by an octahedral tilting around $\vec{b}$ and $\vec{a}$ axes of the orthorhombic unit cell. In the case of the $a_+^-\ b_0^0\ a_-^-$ configuration, the tilting does not change the length of the parameter *a* and reduces *b*, whereas for the $a_+^-\ b_0^0\ a_+^-$ configuration, the situation is inverse. In regard to the requirement of a tetragonal metric ($a/2 = b$), the former tilt configuration seems certainly more preferable. This conclusion is at variance with the widely accepted view that the crystal symmetry of PZ is described by the *Pbam* space group. It must be pointed out that these two possibilities are indistinguishable on the basis of only a powder diffraction experiment. Both space groups are characterized by the same $2\sqrt{2}a_p \times \sqrt{2}b_p \times 2c_p$ unit cell. The difference is in weak

Table 2. Atomic Coordinates and Isotropic Thermal Parameters (B_{iso}) for $BiMg_{1/2}Ti_{1/2}O_3$ at Room Temperature[a]

atom	position	occupancy	*x*	*y*	*z*	B_{iso} (Å^2)
Bi1	4*g*	1	-0.3729(12)	0.2803(19)	0.5	1.31(14)
Bi2	4*g*	1	0.1289(15)	0.7925(21)	0.5	0.94(12)
Ti	8*h*	0.5	-0.3781(39)	0.2425(31)	0.7565(180)	0.01(37)
Mg	8*h*	0.5	-0.3781(39)	0.2425(31)	0.7565(180)	0.01(37)
O1	4*g*	1	0.1299(114)	0.3352(51)	0.5	0.42(56)
O2	4*g*	1	0.6201(85)	0.3249(50)	0.5	0.47(52)
O3	8*h*	1	0.2499(46)	0.5197(73)	0.8199(71)	0.97(35)
O4	4*e*	1	0	0	0.6950(52)	0.13(41)
O5	4*f*	1	0	0.5	0.8100(50)	0.48(39)

[a] Space group *Pnnm*; cell parameters: $a = 11.3207(10)$ Å, $b = 5.6433(10)$ Å, $c = 7.8314(10)$ Å, $V = 500.32(12)$ Å^3; $Z = 8$; $D_{calcd} = 7.781$ g/cm^3. Reliability factors: $R_p = 7.16\%$, $R_{wp} = 9.41\%$, $\chi^2 = 4.99$.

Table 3. Atomic Coordinates and Isotropic Thermal Parameters (B_{iso}) for $BiMg_{1/2}Ti_{1/2}O_3$ at Room Temperature[a]

atom	position	occupancy	x	y	z	B_{iso} (Å^2)
Bi1	4*g*	1	-0.3728(11)	-0.2976(18)	0	0.86(11)
Bi2	4*h*	1	0.1293(13)	0.7925(16)	0.5	1.52(14)
Ti	8*i*	0.5	-0.3789(40)	0.2424(31)	0.7481(159)	0.22(43)
Mg	8*i*	0.5	-0.3789(40)	0.2424(31)	0.7481(159)	0.22(43)
O1	4*g*	1	0.1654(47)	0.2519(151)	0	1.61(51)
O2	4*h*	1	0.5876(39)	0.2458(141)	0.5	1.46(45)
O3	8*i*	1	0.2483(48)	0.4824(82)	0.6800(54)	1.32(31)
O4	4*e*	1	0	0	0.8190(46)	0.32(39)
O5	4*f*	1	0	0.5	0.8073(46)	0.41(42)

[a] Space group *Pbam*; cell parameters: $a = 11.3196(10)$ Å, $b = 5.6423(10)$ Å, $c = 7.8314(10)$ Å, $V = 500.14(12)$ Å^3; $Z = 8$; $D_{calcd} = 7.784$ g/cm^3. Reliability factors: $R_p = 7.14\%$, $R_{wp} = 9.38\%$, $\chi^2 = 4.97$.

superstructure reflections, with $l = 2n + 1$ originating from oxygen displacements. In the case of the $a^-_+ b^0_0 a^-_+$ tilt configuration (*Pbam*), a set of the reflections $\{h\ 0\ l;\ h = 2n\}$ (in the orthorhombic unit cell indication) should be present, whereas for the $a^-_+ b^0_0 a^-_-$ configuration, (*Pnnm*) the respective reflections are $\{0\ k\ l;\ k = 2n + 1\}$. Because of a tetragonal metric of the pseudocubic subcell resulting in the $a/2 = b$ ratio, these reflections superpose in a powder diffraction pattern. It could be supposed that the space group for PZ was determined wrongly; however, the same conclusion was drawn by Glazer et al.[27] and Corker et al.[28] on the basis of a single-crystal diffraction. Moreover, the authors of ref 27 paid special attention to the search for 0−odd−odd type of reflections (odd−0−odd in their setting with the long *b*-axis, $\sqrt{2}a_p \times 2\sqrt{2}b_p \times 2c_p$). At the same time, they have considered no likely mechanism that could promote a tetragonal metric of the PZ pseudocubic subcell.

Because the actual symmetry of BMT could not be unambiguously stated from the available diffraction experiment and the metric arguments on the basis of the rigid tilting of the octahedra do not always work well,[29,30] its powder XRD pattern was refined using both *Pbam* and *Pnnm* space groups. The structural parameters obtained in the refinement are summarized in Table 2 and 3, respectively. The starting models were generated by ISOTROPY from the 1*a*, 1*b* and 3*d* Wyckoff positions in the parent $Pm\bar{3}m$ space group and the $R_4^+ \oplus \sum_2$ reducible representation with an appropriate direction of the coupled order parameter.

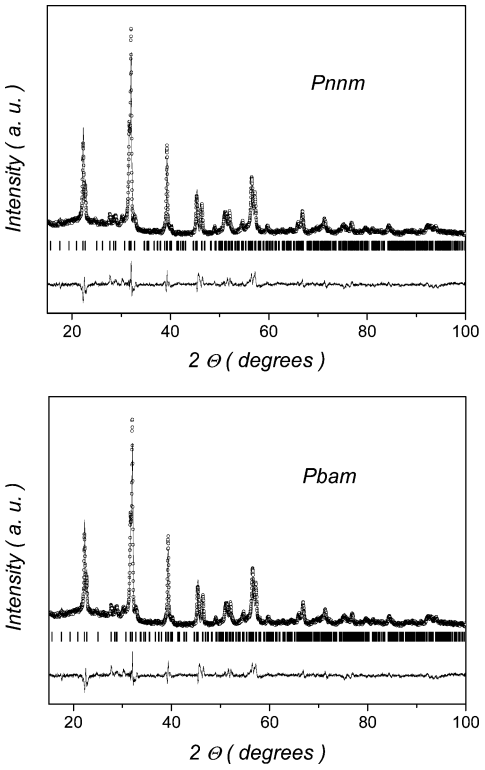

Figure 6. Observed (circles), calculated (continuous curve), and difference (solid line below the spectrum) room-temperature X-ray powder diffraction pattern of BMT. The vertical bars correspond to the calculated peak positions. The refinement was performed in both *Pnnm* (top) and *Pbam* (bottom) space groups.

The refinement of the oxygen positions was performed in two stages. At the beginning, to obtain a first approximation for the crystal structure, we applied a set of constraints. These were deduced from the assumption concerning rigid octahedra tilted in a $a^-_+ b^0_0 a_+{}^-/a^-_+ b^0_0 a^-_-$ configuration. The first

(27) Glazer, A. M.; Roleder, K.; Dec, J. *Acta Crystallogr., Sect. B* **1993**, *49*, 846.
(28) Corker, D. L.; Glazer, A. M.; Dec, J.; Roleder, K.; Whatmore, R. W. *Acta Crystallogr., Sect. B* **1997**, *53*, 135.
(29) Wong, T. K.-Y.; Kennedy, B. J.; Howard, C. J.; Hunter, B. A.; Vogt, T. *J. Solid State Chem.* **2001**, *156*, 255.
(30) Howard, C. J; Withers, R. L.; Kennedy B. J. *J. Solid State Chem.* **2001**, *160*, 8.

parameter taken with an appropriate sign varied the *z*-component for the O3−O5 atoms. The second varied *x*- and *y*-components for O1 and O2 in the case of the *Pbam* and *Pnnm* space groups, respectively. Other oxygen displacement parameters unconstrained by the symmetry but not required by the $a^-_+ b^0_0 a^-_+/a^-_+ b^0_0 a^-_-$ tilted configurations to be changed were fixed. In the second stage, the refinement was allowed to progress without any constraints. The crystal structure data (bond distances and angles) evaluated from the refined atomic positions are presented in the Supporting Information.

As expected, no difference in the XRD patterns of BMT refined using either the *Pbam* or *Pnnm* space group was revealed (Figure 6). In both cases, the fitting procedure yielded similar values of the reliability factors (cf. Tables 2 and 3). Nevertheless, on the basis of the above considered combinations of the *A*-cation displacement and the antiphase octahedral tilting with respect to the observed tetragonal metric, one can conclude that the *Pnnm* space group is the most adequate for description of the crystal structure of BMT.

It was also found from the refinement that Bi^{3+} cations are displaced on average by ∼0.21 Å from their high-symmetry positions. This value is comparable with the antiferroelectric shift of Pb^{2+} cations in PZ (∼0.23 Å) at room temperature.[27] Preliminary dielectric measurements have revealed an anomaly in the temperature dependence of the dielectric permittivity of BMT; in the vicinity of 700 K, it looked like there was a first-order phase transition. However, a conclusion concerning the type of a dipole ordering in BMT cannot be drawn until the detailed dielectric studies have been carried out. These investigations are in progress and will be reported elsewhere.

Conclusions

Single-phase ceramics of the $Bi(Mg_{1/2}Ti_{1/2})O_3$ composition have not been obtained at normal pressure regardless of what thermal treatment conditions and precursors were used. The perovskite BMT has been synthesized at about 6 GPa and 1270 K. The high-pressure perovskite phase was found to be metastable and decompose when annealing at temperatures as low as 1020 K.

X-ray and electron diffraction experiments performed on the ceramics that annealed below the decomposition temperature revealed a superstructure associated with both the antiferroelectric-like displacements of Bi^{3+} cations and the antiphase tilting of oxygen octahedra. A detailed examination of the observed superstructure in combination with a group theoretical analysis of possible distortional configurations has resulted in the conclusion that the crystal structure of the BMT perovskite can be described using either the *Pnnm* or *Pbam* space group ordinarily attributed to antiferroelectric PZ. On the basis of the powder diffraction experiment only, these two possibilities are indistinguishable. Nevertheless, reasoning from the likely mechanism promoting a tetragonal metric of the primitive unit cell of BMT, we believe the actual crystal symmetry of BMT to be characterized by the *Pnnm* space group.

Acknowledgment. The authors acknowledge the Foundation for Science and Technology (FCT-Portugal; Grants SFRH/BPD/12669/2003, SFRH/BPD/14988/2004, and SFRH/BPD/15004/2004) as well as the Belarusian Republican Fund for Fundamental Researches (Φ05MC-013) for their financial support.

CM061129W